AE23A-0900

Sprite-attributed infrasonic chirps FROM THUNDERSTORMS

Ludwik Liszka
Swedish Institute of Space Physics
SE-90187 Umeå, Sweden
E-mail: ludwik@irf.se

Carl-Fredrik Enell
Sodankylä Geophysical Observatory
Sodankylä, Finland
E-mail: carl-fredrik.enell@sgo.fi

Abstract

During the past 13 years, sprite-attributed infrasonic chirps were recorded at infrasonic arrays managed by the Swedish-Finnish Infrasound Network. This study is concentrated on the morphology of the phenomenon, in particular on its temporal and spatial distributions. The occurrence of chirps reveals a 3.2-year variation, which is in phase with the corresponding component of solar activity. Daily- and annual variations indicate that the phenomenon does not necessarily coincide with the local thunderstorm activity.
In addition to a conventional wavelet analysis, the chirps were analyzed using a set of 6 wavelet filters covering the frequency band 0.5 – 6 Hz. A representation of the chirp in the angle-of-arrival – frequency domain (AoA-F) describes both the source and the influence of the atmosphere on the chirp signal. It provides information about the horizontal extent of the source. The AoA-F representation may be used for categorization of the phenomenon. Also the horizontal trace velocity of the chirp signal is studied in the frequency domain. It provides information about the angle of incidence of the ray at different frequencies and thus about the vertical extent of the source.

Introduction

Since the end of 1994, four infrasonic arrays, with a continuous storage of recorded time series, were in operation in Sweden (see Table 1 and Fig 1). In October 2006, the Uppsala array was moved to Sodankylä in Northern Finland.

Name	Latitude (Degrees)	Longitude (Degrees)
Kiruna	67.8˚N	20.4˚E
Jämtön	65.87˚N	22.51˚E
Lycksele	64.61˚N	18.71˚E
Uppsala	59.85˚N	17.61˚E

Table 1: Stations in the Swedish-Finnish Infrasound Network.

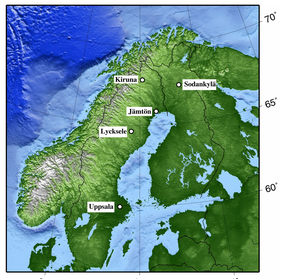

Fig 1: Location of infrasound stations in Sweden and Finland.

Data from all arrays are continuously analyzed using a cross-correlation method. The analyzed signals are band-pass-filtered in the frequency range 0.5 – 6 Hz. Recently, filtered data in six narrow frequency bands have been used. The detection criterion is based on the value of the product, ρ, of all three correlation coefficients in the array. Calculated values of the angle-of-arrival, A, and of the horizontal trace velocity, Vp, are assumed significant for ρ≥0.02.

Morphology of sprite-generated infrasonic chirps

The sprite-attributed infrasonic chirps were discovered in connection with an unusual intense system of thunderstorms on May 26, 1995 (Liszka, 2001). The chirp consists of a low frequency sound wave, starting at approximately 1 – 2 Hz and increasing to about 5 – 8 Hz. Frequently, there are additional pulses of higher frequency (~6 Hz) before and after the chirp (see Fig 3, right graph). This peculiar signature is a result of the dispersion of the signal in the wind- and temperature distribution in the atmosphere. The chirp signature is most clearly visible across the dominating winds and in particular from the north side of the sprite discharge. Additional information about the nature of the chirp may be obtained filtering all the signals from the array with a set of band-pass filters (see Table 2 and Fig 2).

Frequency band #	Frequency, Hz	Type of filter	Centre frequency, Hz
1	<1	Low-pass	.75
2	1 – 2	Band-pass	1.5
3	2 – 3	"	2.5
4	3 – 4	"	3.5
5	4 – 5	"	4.5
6	>5	High-pass	5.5

Table 2: List of wavelet filters

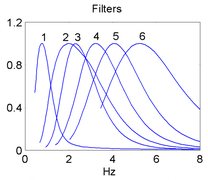

Fig 2: Transmission curves for wavelet filters.

Since the microphone signal is band-pass filtered between 0.5 and 6 Hz, the center frequencies of channels 1 and 6 may be estimated to 0.75, respective 5.5 Hz.

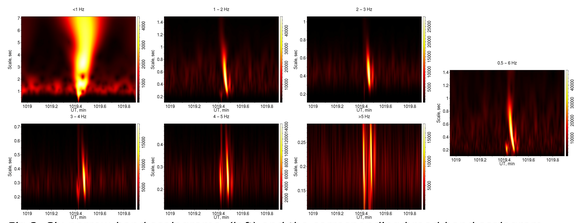

Fig 3: Six narrow-band scalograms (left) and the corresponding broad-band scalogram (right). Observe different scales on both Y- and Z-axis.

In addition to the scalogram of the broad-band signal (0.5 – 6 Hz), six scalograms of outputs from individual filters may be calculated. An example of six narrow-band scalograms (left) and the corresponding broad-band scalogram (right) is shown in Fig 3.

Each point of the scalogram is associated with a pair of values of the angle-of-arrival and of the horizontal trace velocity obtained from correlation analysis of filtered signals.
The multi-frequency analysis results in a representation of the chirp in the angle-of-arrival – frequency domain. It describes both the source and the influence of the atmosphere on the chirp signal. It provides information about the horizontal extent of the source. The AoA-F representation may also be used for categorization of the phenomenon. Also the horizontal trace velocity of the chirp signal is studied in the frequency domain. It provides information about the angle of incidence of the ray at different frequencies and thus about the vertical extent of the source.
Examples of the broad-band scalogram together with the multi-frequency analysis are shown in Figs. 4 – 7.

Fig 4: A sequence of chirps (left) arriving from approximately the same direction (middle). The complex distribution of trace velocities (right) indicates signals arriving at different ray inclinations.

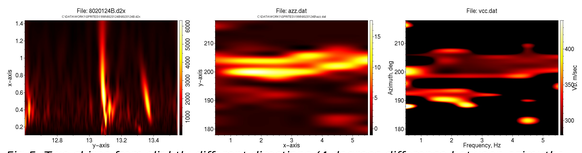

Fig 5: Two chirps from slightly different directions (4 degrees difference between azimuths throughout the entire frequency range). The trace velocity graph indicates a third weaker component from a direction of 190-192 degrees.

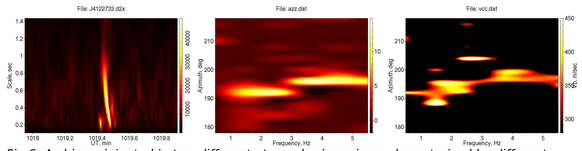

Fig 6: A chirp originated in two different atmospheric regions, characterized by different wind velocities. The low frequency component on the middle graph corresponds to higher altitude, with a stronger eastward wind, necessary to get a lateral deviation of 3 degrees with respect to the higher frequency component.

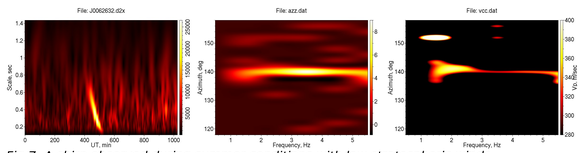

Fig 7: A chirp observed during summer conditions with low stratospheric winds.

The discontinuity seen in the angle-of-arrival – frequency graph in Figs. 4 – 6 reflects the structure of the vertical distribution of atmospheric winds, since the dominating frequency corresponds to a specific height interval (cf. Fig 2).

Geographical occurrence of sprite-attributed chirps

Earlier work (Liszka, 2003, 2004 and Liszka & Hobara, 2006) indicates that most of the chirps observed from the Jämtön-array are located along the coastlines of the Gulf of Bothnia, in particular over its narrowest part (Kvarken-area). Most of chirps were observed only at one array (Jämtön). In cases when it was possible to identify the same event from another array (Lycksele) the result of triangulation also indicates the coastal area, see Fig 8.

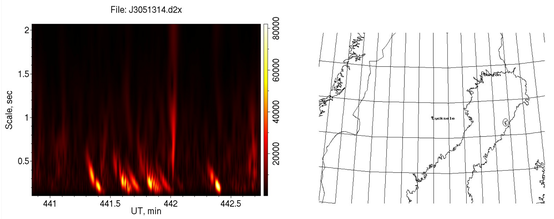

Fig 8: A sequence of chirps and their localization from arrays in Jämtön and Lycksele (encircled on the map).

Occurrence of sprite-attributed chirps – temporal variations

The vast majority of sprite-attributed infrasonic chirps observed over Northern Scandinavia are recorded at the Jämtön-array. The probable reason for that was discussed earlier (Liszka & Hobara, 2006). There is a distinct temporal variation of the chirps observed at the Jämtön-array. The yearly numbers of observations are shown in Fig 9. It must be remembered that some events consist of a series of close chirps, which are counted as a single event in the statistics. An example is shown in Fig 4.

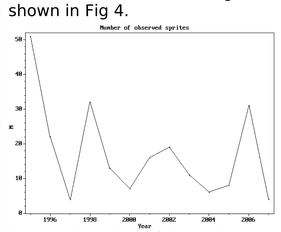

Fig 9: Yearly numbers of observed sprite-attributed infrasonic chirps. It must be remembered that the large part of chirps (31) in 1995 occurred during the same night of May 26, in connection with a large thunderstorm system.

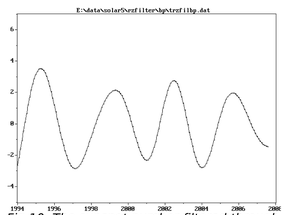

Fig 10: The sunspot number filtered through a wavelet band-pass filter 35-45 months (around 3.25 years)

There is an apparent similarity between the graph in Fig 9 and the sunspot number filtered by a band-pass wavelet filter centred at 3.2 years (see Fig 10). That component of solar activity appears to be in phase with the number of recorded chirps shown in Fig 9.

A comparison with the thunderstorm activity during the same period is illustrated in , showing the number of thunderstorms recorded per year by the Lycksele-array, closest to the Kvarken-area, where the majority of chirps are observed.

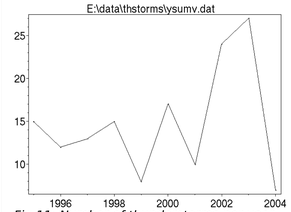

Fig 11: Number of thunderstorms per year recorded at the Lycksele-array.

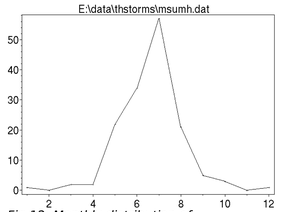

Fig 12: Monthly distribution of thunderstorms recorded at the Lycksele-array during 1995-2004.

However, the distribution of thunderstorms and infrasonic chirps throughout the year is completely different (Figs. 12 and 13).

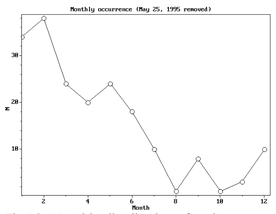

Fig 13: Monthly distribution of sprite-attributed infrasonic chirps at the Jämtön-array during 1995-2007. Events of May 26, 1995 are removed from the statistics.

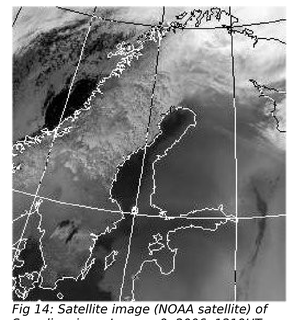

Fig 14: Satellite image (NOAA satellite) of Scandinavia on January 9, 2006, 1219UT.

The above observation is astonishing. The number of observed chirps has a distinct maximum during the winter months, contrary to the number of thunderstorms observed in this area. The observation could be in agreement with the hypothesis about conjugate sprites (http://www-star.stanford.edu/~vlf/southafrica/southafrica.htm). According to this hypothesis sprites could be generated by thunderstorm activity at the magnetic conjugate area in the opposite hemisphere. The conjugated point to the Kvarken-area is located over the sea, south-east of Crozet Islands and south-west of Kerguelen Island . The local summer occurs there during December – February, when most of infrasonic chirps are observed in Scandinavia. At several occasions, when infrasonic chirps were observed over the Gulf of Bothnia, there was not a single cloud over the area (see example of Fig 14).

Diurnal occurrence of sprite-attributed chirps

Since the data are stored in 30-minute files, it was convenient to count the number of observed chirps during each 30-minute period (0 – 47). The resulting counts are displayed in Fig 15. The statistics covers the period January 1995 – June 2007. Counts are plotted as a function of UT.

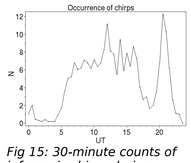

Fig 15: 30-minute counts of infrasonic chirps during January 1995 – June 2007 plotted as a function of UT. The evening peak is due to a single, local thunderstorm on May 26, 1995

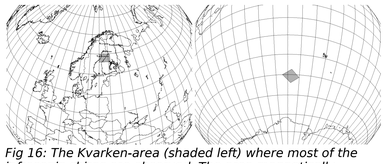

Fig 16: The Kvarken-area (shaded left) where most of the infrasonic chirps are observed. The area magnetically conjugated to the Kvarken-area shown right.

The evening peak is due to a single, local thunderstorm on May 26, 1995. The local noon in the area, conjugated to the area where the majority of chirps are observed (see Fig 16), occurs between 0800 and 0830 UT. The position of the conjugated area has been calculated using the GSFC NASA on-line coordinate transformation facility (http://modelweb.gsfc.nasa.gov/models/cgm/cgm.html), which is herewith acknowledged.

Conclusions

Multi-frequency analysis of infrasonic chirps provides information about both the morphology of the source itself and about the influence of the surrounding atmosphere upon the propagation of recorded signals. A detailed morphological study of the chirps will be the subject of a separate publication.
A 12-year statistics of infrasonic chirps indicates that, at least a part of them, is a winter-time phenomenon and thus not connected with local thunderstorms. The hypothesis about sprites generated by thunderstorms at magnetically conjugate points is in agreement with the observed statistics.

References

Liszka, L.: On the Possible Infrasound Generation by Sprites. Paper presented at the AGU Fall Meeting, 2003, San Francisco.

Liszka, L., 2004: On the possible infrasound generation by sprites, *Journ. of Low Frequency Noise, Vibration and Active Control*, *23*, 85-93.

Liszka, L. & Y. Hobara, 2005: Sprite-attributed infrasonic chirps – their detection, occurrence and properties between 1994 and 2004, Journ. *of Atmospheric and Solar-Terrestrial Physics*, 68, 1179-1188.